J Nanopart Res (2012) 14:704
DOI 10.1007/s11051-011-0704-5

RESEARCH PAPER

Immobilization of platinum nanoparticles on 3,4-diaminobenzoyl-functionalized multi-walled carbon nanotube and its electrocatalytic activity

Hyun-Jung Choi · Ji-Ye Kang · In-Yup Jeon · Soo-Mi Eo · Loon-Seng Tan · Jong-Beom Baek

Received: 17 July 2011 / Accepted: 26 December 2011 / Published online: 26 January 2012

Abstract Multi-walled carbon nanotubes (MWCNTs) are functionalized at the sp^2 C–H defect sites with 3,4-diaminobenzoic acid by a "direct" Friedel–Crafts acylation reaction in a mild polyphosphoric acid/phosphorous pentoxide medium. Owing to enhanced surface polarity, the resulting 3,4-diaminobenzoyl-functionalized MWCNTs (DAB-MWCNT) are highly dispersible in polar solvents, such as ethanol, *N*-methyl-2-pyrrolidone, and methanesulfonic acid. The absorption and emission properties of DAB-MWCNT in solution state are qualitatively shown to be sensitive to the pH in the environment. The DAB-MWCNT is used as a stable platform on which to deposit platinum nanoparticles (PNP). The PNP/DAB-MWCNT hybrid displays high electrocatalytic activity with good electrochemical stability for an oxygen reduction reaction under an alkaline condition.

Keywords Platinum nanoparticles · Multi-walled carbon nanotubes · Functionalization · Electrocatalytic activity

Electronic supplementary material The online version of this article (doi:10.1007/s11051-011-0704-5) contains supplementary material, which is available to authorized users.

H.-J. Choi · J.-Y. Kang · I.-Y. Jeon · S.-M. Eo · J.-B. Baek (✉)
Interdisciplinary School of Green Energy/Institute of Advanced Materials and Devices, Ulsan National Institute of Science and Technology, Ulsan 689-798, South Korea
e-mail: jbbaek@unist.ac.kr

L.-S. Tan
Nanostructured and Biological Materials Branch (AFRL/RXBN), Materials and Manufacturing Directorate, Air Force Research Laboratory, Wright-Patterson AFB, Dayton, OH 45433, USA

Introduction

Carbon nanotubes (CNTs) have attracted a lot of attention because of their excellent mechanical, thermal, and electrical properties, and chemical stability, stemming from their unique elongated fullerene structure (Tasis et al. 2006). CNTs are good candidates as advanced materials such as nanoscale reinforcing additives (Carneiro et al. 1998) and catalytic supports (Lee et al. 2005; Shi et al. 2009; Alexeyeva et al. 2010). More recently, in a research directed to combine the advantages of CNTs and metal nanoparticles, various approaches to generating such hybrid systems have been reported, such as physical evaporation (Yu et al. 1998), thermal reduction of adsorbed metal salts under H_2 atmosphere (Xue et al. 2001), "wet" reduction of metal salts adsorbed on surface-oxidized CNTs (Li et al. 2003), redox reaction between metal ions and reduced CNT (Lorenc on et al. 2009), nanoscale electroless metal deposition process (Li et al. 1998), and assembly of CNT–metal nanoparticle hybrids using biointerfaces (Kim et al. 2010). Among these options, the deposition of

Report Documentation Page

Form Approved
OMB No. 0704-0188

1. REPORT DATE	2. REPORT TYPE	3. DATES COVERED
26 JAN 2012		**00-00-2012 to 00-00-2012**

4. TITLE AND SUBTITLE	5a. CONTRACT NUMBER
Immobilization of platinum nanoparticles on 3,4-diaminobenzoyl-functionalized multi-walled carbon nanotube and its electrocatalytic activity	5b. GRANT NUMBER
	5c. PROGRAM ELEMENT NUMBER
6. AUTHOR(S)	5d. PROJECT NUMBER
	5e. TASK NUMBER
	5f. WORK UNIT NUMBER
7. PERFORMING ORGANIZATION NAME(S) AND ADDRESS(ES) **Ulsan National Institute of Science and Technology (UNIST),Interdisciplinary School of Green Energy & Inst of Advanced Materials & Devices,100, Banyeon,Ulsan 689-798, South Korea,**	8. PERFORMING ORGANIZATION REPORT NUMBER
9. SPONSORING/MONITORING AGENCY NAME(S) AND ADDRESS(ES)	10. SPONSOR/MONITOR'S ACRONYM(S)
	11. SPONSOR/MONITOR'S REPORT NUMBER(S)

12. DISTRIBUTION/AVAILABILITY STATEMENT
Approved for public release; distribution unlimited

13. SUPPLEMENTARY NOTES

14. ABSTRACT
Multi-walled carbon nanotubes (MWCNTs) are functionalized at the sp2 C?H defect sites with 3,4-diaminobenzoic acid by a ??direct?? Friedel?Crafts acylation reaction in a mild polyphosphoric acid/ phosphorous pentoxide medium. Owing to enhanced surface polarity, the resulting 3,4-diaminobenzoylfunctionalized MWCNTs (DAB-MWCNT) are highly dispersible in polar solvents, such as ethanol N-methyl-2-pyrrolidone, and methanesulfonic acid. The absorption and emission properties of DABMWCNT in solution state are qualitatively shown to be sensitive to the pH in the environment. The DABMWCNT is used as a stable platform on which to deposit platinum nanoparticles (PNP). The PNP/DABMWCNT hybrid displays high electrocatalytic activity with good electrochemical stability for an oxygen reduction reaction under an alkaline condition.

15. SUBJECT TERMS

16. SECURITY CLASSIFICATION OF:			17. LIMITATION OF ABSTRACT	18. NUMBER OF PAGES	19a. NAME OF RESPONSIBLE PERSON
a. REPORT **unclassified**	b. ABSTRACT **unclassified**	c. THIS PAGE **unclassified**	**Same as Report (SAR)**	**11**	

nanoparticles onto the surface-functionalized CNTs is perhaps the most reliable for performance, reproducibility, and scalability (Xue et al. 2001; Li et al. 2003; Lorenc on et al. 2009). The dispersion and functionalization of raw CNTs have been typically carried out by sonication (Shaffer and Windle 1999; Chen et al. 2000) in strong acids such as sulfuric acid and nitric acid (Sun et al. 2002; Dai and Mau 2001; Hirsch 2002), or sonication in strong acid mixtures (Li et al. 2003; Zhang et al. 2000; Huang et al. 2002). However, it is generally known that such treatments could result in structural damage to the CNTs (Heller et al. 2005). As a result, the CNTs would lose valuable characteristics such as their electrical properties and structural integrity after introducing various oxygenated groups into their framework. The oxidized defects on the CNTs are probable sites for deactivation of transition metal catalysts (Wildgoose et al. 2006). Hence, the development of a simple and benign process for functionalization becomes more important for the CNTs without and/or with minimal damages (Han et al. 2008; Lee et al. 2008).

We have developed a non-oxidizing and less destructive method that combines purification and functionalization of carbon-based nanomaterials in a single-pot process utilizing polyphosphoric acid (PPA) with additional phosphorous pentoxide (P_2O_5), which plays the roles of a solvating/dispersing medium and a Brönsted catalyst for Friedel–Crafts acylation of carbon nanomaterials (Baek et al. 2004). PPA is a polymeric form of phosphoric acid (H_3PO_4, $pK_a \sim 2.1$), which is less corrosive and practically non-oxidizing as compared with commonly used strong acids (HNO_3, $pK_a \sim -1.3$; H_2SO_4, $pK_a \sim -3.0$). Commercial grade PPA (83% P_2O_5 assay) has been used as a polymerization medium for the synthesis of high-performance polybenzazoles (PBXs) (Eo et al. 2008; Wolfe 1988). If the purification and functionalization of CNTs could be achieved in a non-destructive and one-pot fashion, then it would be an ideal system to exploit.

In this study, multi-walled carbon nanotubes (MWCNTs) were functionalized with 3,4-diaminobenzoic acid (DABA) via "direct" Friedel–Crafts acylation reaction to produce covalently 3,4-diaminobenzoyl-functionalized MWCNT (DAB-MWCNT). Platinum nanoparticle (PNP), is a known catalyst for hydrogenation and Heck reactions that can bind strongly amine groups (Mandal et al. 2004). It is believed that PNP can be stably anchored to DAB-MWCNT without agglomeration. Thus, the resulting PNP/DAB-MWCNT hybrid is expected to have high electrocatalytic performance with good electrochemical stability.

Experimental

Materials

All reagents and solvents were purchased from Aldrich Chemical Inc., USA and were used as received, unless otherwise specified. MWCNT (CVD MWCNT 95 with a diameter of $\sim$20 nm and a length of 10–50 μm) was obtained from Hanwaha Nanotech Co., LTD, Seoul, Korea. The commercial grade platinum on the activated carbon catalyst (Pt/C, C2–20, 20% HP Pt on Vulcan XC-72R, E-TEK Division, PE-MEAS Fuel Cell Technologies) was provided by BASF Fuel Cell.

Instrumentation

The Fourier-transform infrared (FT-IR) spectra were recorded on a Jasco FT-IR 480 plus spectrophotometer. Solid samples were imbedded in KBr disks. Elemental analysis (EA) was performed using a CE Instrument EA1110. Thermogravimetric analysis (TGA) was conducted in an air atmosphere with a heating rate of 10 °C·min^{-1} using a TA Q200. Wide-angle X-ray diffraction (WAXD) powder patterns were recorded using a Rigaku RU-200 diffractometer applying Ni-filtered Cu Kα radiation (40 kV, 100 mA, $\lambda = 0.15418$ nm). The field emission scanning electron microscopy (FE-SEM) used in this study was performed using an FEI NanoSem 230. High-resolution transmission electron microscopy (HR-TEM) in this study was performed using a JEOL JEM-2100F (Cs) operating at 200 kV. Photoluminescence measurements were performed using a Perkin-Elmer LS 55 fluorescence spectrometer. Stock solutions were prepared by dissolving 20 mg of each sample in 5 mL (4 mg·mL^{-1}) of methanesulfonic acid (MSA) or *N*-methyl-2-pyrrolidone (NMP). The excitation wavelength was that of the UV absorption maximum of each sample.

For electrochemical measurements, cyclic voltammetry (CV) was carried out using a VersaSTAT3

AMETEK model (Princeton Applied Research, TN, USA) potentiostat/galvanostat employing a standard three-electrode electrochemical cell. This consisted of samples on glassy carbon (GC) with a diameter of 3 mm as the working electrode, an Ag/AgCl (saturated KCl) reference electrode, and platinum gauze as the counter electrode. Experiments were carried out at room temperature in a 0.1 M aqueous KOH electrolyte solution. Either nitrogen or oxygen gas was used to purge the solution to achieve an oxygen-free or an oxygen-saturated electrolyte solution, respectively. All potentials are reported relative to an Ag/AgCl (saturated KCl) reference electrode recorded at a scan rate of 10 $mV \cdot s^{-1}$. The potential window for cycling was confined between −1.0 V and +0.2 V in a basic electrolyte to omit the extra current generated by samples in the alkaline medium. The GC electrode was polished with alumina slurry before use to obtain a mirror-like surface. Samples (2.0 mg) were dispersed in NMP (0.2 mL), and aliquots of the suspension (10 μL) were coated on GC electrodes and dried under reduced pressure (0.5-mm Hg) for 24 h at 50 °C. Nafion (5%, 5 μL) in ethanol was pipetted onto the sample/GC electrode and allowed to dry at laboratory conditions for 2 h. Electrodes for rotating disk electrode (RDE) voltammogram measurements were prepared ona 3 mm diameter GC disk electrode (ALS, Japan).

Synthesis of 3,4-diaminobenzoyl-functionalized MWCNT (DAB-MWCNT)

3,4-Diaminobenzoic acid (5.0 g, 31.02 mmol), MWCNT (5.0 g), PPA (83% P_2O_5 assay; 200.0 g) and P_2O_5 (40.0 g) were placed in a 250-mL resin flask equipped with a high torque mechanical stirrer, nitrogen inlet and outlet, and stirred under dry nitrogen purge at 80 °C for 1 h. The temperature was increased incrementally to 100 °C over 1 h. Then, the reaction mixture was stirred at 130 °C for an additional 72 h. At the end of the reaction, the mixture was cooled to room temperature, and distilled water was added. The precipitates were isolated and Soxhlet-extracted with water for 3 days to completely remove the reaction medium and then with methanol for three more days to remove other possible impurities. The final product was freeze-dried under reduced pressure (0.05 mm Hg) for 48 h producing 9.3 g (98%) of black lump of DAB-MWCNT, which could be easily broken up. Found: C, 79.17%; H, 1.93%; N, 8.31%, and O, 5.67%.

Preparation of thin DAB-MWCNT paper via solution casting

Film was cast from DAB-MWCNT (1.0 g) dispersed in MSA, 20 mL. The resultant homogeneous solution was cast on a leveled glass plate in a custom-made film-casting apparatus. MSA was slowly removed by heating the apparatus to 80 °C under reduced pressure (0.05 mm Hg). The resultant film was removed from the glass plate after immersion in distilled water. The free-standing films were sandwiched between Teflon membranes to keep them pressed, and then kept under distilled water for 4 days. The film was further Soxhlet-extracted with water for 3 days and then methanol for an additional 3 days to ensure complete removal of residual MSA. FT-IR spectra of the DAB-MWCNT film were obtained from a crushed sample that was imbedded in KBr pellet and showed that there was no trace of residual MSA by judging the absence of $\nu(SO_2)$ for MSA at 1,202 (symmetric stretching) and 1,403 (asymmetric stretching) cm^{-1}. The average DC conductivity of the cast film was 280 ± 8 S m^{-1}.

In situ synthesis of PNP/DAB-MWCNT hybrid

The PNP was prepared according to the procedure described by Ahmadi et al. (1996). In short, an aqueous solution, containing 18.4 mL of DI water, 0.5 mL of an aqueous 0.05 M $H_2PtCl_6 \cdot 6H_2O$ solution, and 0.5 mL of an aqueous 0.05 M trisodium citrate solution, was mixed in a conical flask. To this solution, an ice-cold aqueous solution (0.6 mL) containing 0.1 M $NaBH_4$ was added in one portion under vigorous magnetic stirring. The solution turned red immediately after the addition of the $NaBH_4$ solution, indicating PNP's formation. DAB-MWCNT (50 mg) was dispersed in 30 mL of ethanol by ultrasonic agitation for 3 min. Then black suspension was added to the solution containing platinum colloids (20 mg) at room temperature. After stirring for 24 h, PNP/DAB-MWCNT hybrids were collected through filtration, washed with water several times, and completely dried under reduced pressure (0.05 mm Hg) at 100 °C for 24 h.

The procedures of GC electrode pretreatment and modification are described as follows: before use, the working electrode was polished with alumina slurry to obtain a mirror-like surface and then washed with DI water and allowed to dry. The samples (1 mg) were dispersed in 1 mL solvent mixture of Nafion (5%) and EtOH/water (v/v = 1:9) by sonication. Each sample suspension (5 μl) was pipetted on the GC electrode surface, followed by drying at room temperature.

Results and discussion

Synthesis of DAB-MWCNT

Table 1 summarizes the EA results. The hydrogen content of a multi-walled carbon nanotube (MWCNT) is 0.30 wt%. The maximum possible ratio of hydrogen/carbon (H/C) is approximately 1/27, which explains the existence of sp^2C–H on the tube defects. Similar to the electrophilic substitution reaction of benzene, the available sp^2C–H is the site for the Friedel–Crafts acylation reaction of MWNCT. Thus, DAB-MWCNT could be prepared from the reaction between DABA and MWCNT in a mild PPA/P_2O_5 medium (Fig. 1) (Lee et al. 2008). Detailed reaction mechanisms are described in the Electronic Supporting Information (ESI, Fig. S1). The advantage of the reaction medium is that it is non-destructive, but strong enough for efficient functionalization compared with typical functionalization by destructive oxidation in nitric acid/sulfuric acid mixtures (Hu et al. 2003). The elemental contents of DAB-MWCNT from EA are consistent with theoretical and experimental values (Table 1).

In order to verify the structure of DAB-MWCNT, FT-IR spectroscopy was commonly used as a convenient tool to trace the chemical modification of carbon nanomaterials (Baek et al. 2004). Since CNTs strongly absorb infrared light, samples have to be carefully prepared to collect reliable spectra. The thinner KBr window gives better resolution. While MWCNT shows a featureless spectrum (Fig. 2a), DAB-MWCNT displays a strong ketone carbonyl (C=O) stretching band at 1,639 cm^{-1}. In addition, DAB-MWCNT also displays distinct C–N stretching band at 1,385 cm^{-1}. Although the N–H stretching bands around 3,430 and 3,350 cm^{-1} are obscured by the more intense and broad O–H stretching band (3,500–3,000 cm^{-1}) of lattice-bound water in the

Table 1 Elemental analysis (EA) data of MWCNT and DAB-MWCNT

Sample	Elemental analysis					
		C (%)	H (%)	N (%)	O (%)	H/C ratio
MWCNT	Calcd.	100.00	0.00	0.00	0.00	0
	Found	97.81	0.30	BDL	0.59	1/27.4
DAB-MWCNT	Calcd.	84.25	1.32	9.17	5.24	1/5.4
	Found	79.17	1.93	8.31	5.67	1/6.6

BDL below detection limit

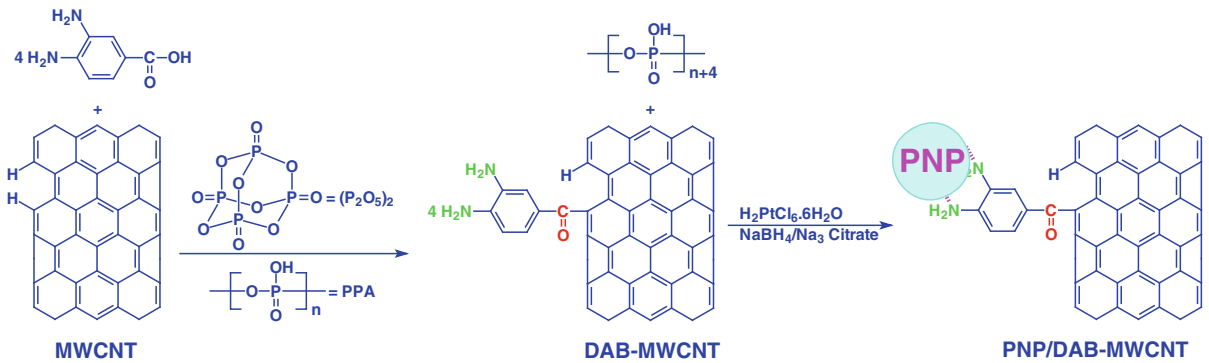

Fig. 1 Functionalization of multi-walled carbon nanotubes (MWCNTs) with DABA to produce DAB-MWCNT and preparation of PNP on DAB-MWCNT (PNP/DAB-MWCNT). Detailed mechanism for the synthesis of DAB-MWCNT is delineated in Fig. S1

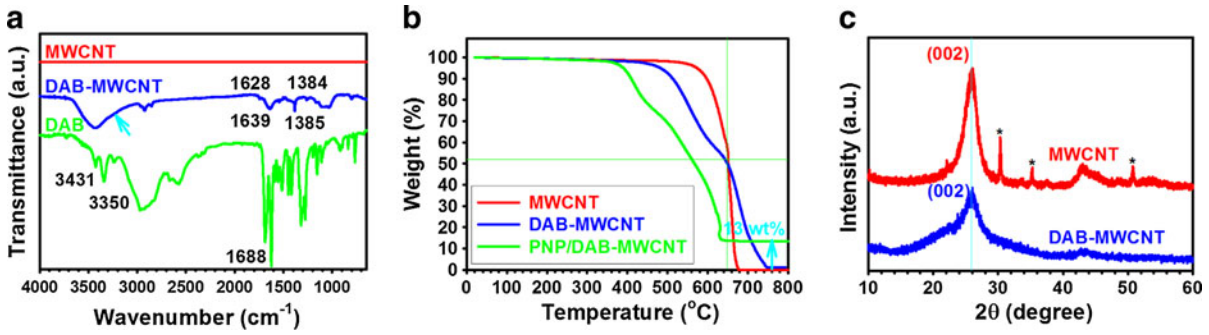

Fig. 2 **a** FT-IR (KBr pellet) spectra. **b** TGA thermograms obtained with heating rate of 10 °C min^{-1} in air. **c** XRD patterns. Metallic impurity peaks have completely disappeared in DAB-MWCNT, while wall-to-wall interlayer peak remains at 26.0° (*d*-spacing = 3.42 Å)

KBr, the right shoulder (Fig. 2b, sky blue oval) from DAB-MWCNTs should be attributed to amine of the N–H stretching band (sky blue arrow).

The degree of functionalization was estimated using TGA in air atmosphere. Since the functionalization is non-destructive, the early weight loss is ascribable to thermo-oxidative decomposition of DAB ($C_7H_7N_2O$, FW = 136.06) moiety. DAB-MWCNT shows a two-step weight loss from ~460 to 800 °C. Initial weight loss from ~460–650 °C was 48 wt%, which is attributed to thermo-oxidative stripping of the DAB moiety (Fig. 2b). The value agreed well with the feed ratio of DAB/MWCNT (1/1, wt/wt) and near-quantitative yield of DAB-MWCNT, indicating high efficiency functionalization. Thus, the degree of functionalization is estimated to be less than 8 atom%.

Furthermore, the role of the reaction medium and morphology of DAB-MWCNT could be evaluated from X-ray diffraction (XRD) patterns. The XRD powder pattern from pristine MWCNT shows the presence of metallic impurities (peaks marked with *), while there are no peaks for impurities in the DAB-MWCNT (Fig. 2c). The result suggests that the reaction medium can purify and functionalize MWCNT at the same time. DAB-MWCNT shows (002) peak at 26.00° (d-spacing = 3.42 Å).

The functionalization could be visually ascertained by scanning electron (SEM) and transmission electron (TEM) microscopes. Pristine MWCNT shows that their surface is clean and smooth with diameters in the range of 10 ~ 20 nm (Fig. 3a). DAB-MWCNT is uniformly coated with DAB moiety, and the average diameter is increased to about 40 ~ 50 nm (Fig. 3b). Magnified images clearly reveal core–shell structure (Fig. 3c). The average diameter of an inner core is approximately 20 nm, and the average thickness of an outer shell is roughly 15 nm (Fig. 3c, inset). Considering the average diameter of pristine MWCNT (10 ~ 20 nm) and the average thickness of DAB layer (~1 nm), the increased thickness should be due to bundling of DAB-MWCNT (Jeon et al. 2008) because the surface polarity of DAB-MWCNT is much higher than that of pristine MWCNT. The enhanced lateral interactions of DAB-MWCNT driven by inter-tube hydrogen bonding after functionalization is strong enough to overcome the rigidity of MWCNT, resulting in the formation of DAB-MWCNT bundles. The result implies that the uniform decoration of DAB onto the surface of MWCNT may be achieved through "direct" Friedel–Crafts acylation reaction in PPA/P_2O_5.

The morphology of DAB-MWCNT could be further assayed by TEM. Again, the surface of pristine MWCNT is apparently clean and smooth (Fig. 4a, b), showing almost no carbonaceous impurity deposits. On the contrary, DAB moiety is uniformly populating the surface of MWCNT (Fig. 4c). Specifically, the tip of the DAB-MWCNT appears to be more DAB-coated (white arrow) because of the possibility of sp^2 C–H defects at the tube end being much higher (Charlier 2002).

DAB-MWCNT is dispersed well in both acidic and basic solvents, e.g., MSA and NMP, respectively, as well as their mixtures. In addition, it is also dispersible in alcohol, probably because of its enhanced surface polarity. The photograph of the DAB-MWCNT in MSA solutions demonstrates its strong ability for dispersal (Fig. 5a, inset). These solutions were

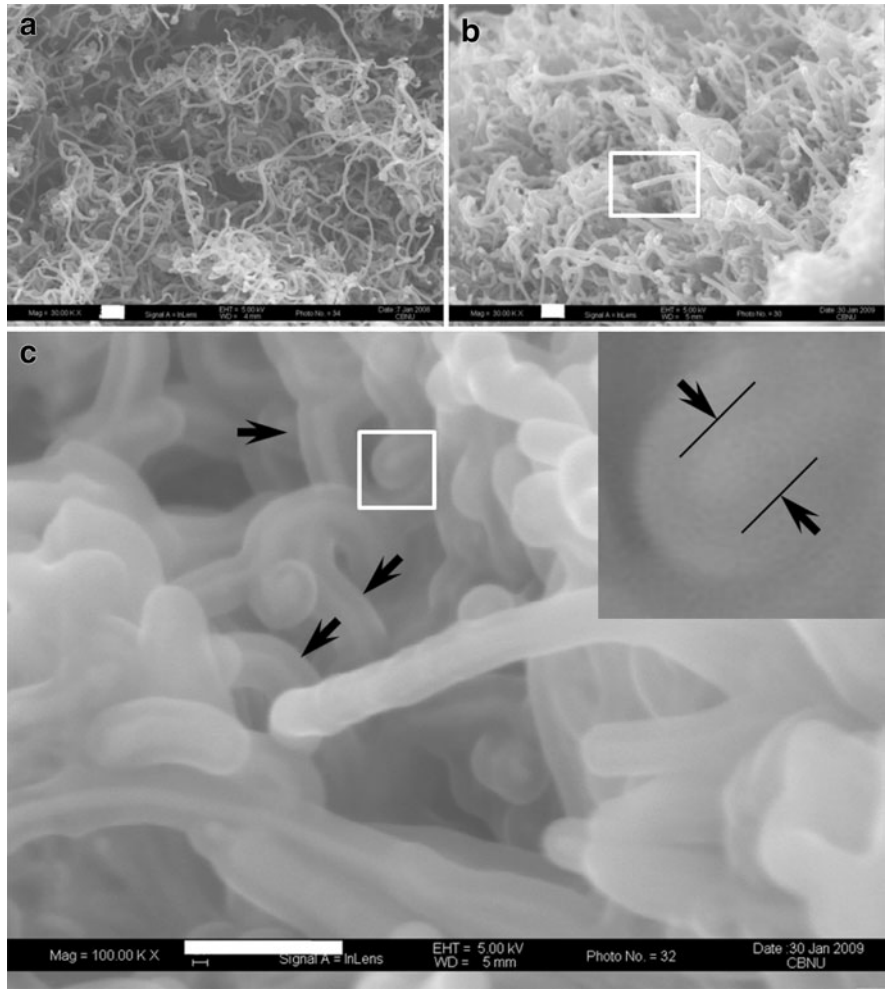

Fig. 3 SEM images of samples: **a** pristine MWCNT. **b** DAB-MWCNT.; **c** magnified image of the rectangle area in (*b*). *Inset* is magnified image from a *white square* in (*c*), showing core–shell structure of DAB-MWCNT. *Scale bars* are 200 nm

homogeneous and transparent, while pristine MWCNT solution contained mostly MWCNT agglomerates (not shown). The DAB-MWCNT displayed different UV-absorption and emission behaviors in different solvents. DAB-MWCNT in an acidic MSA solution had an absorption maximum at 365 nm (Fig. 5a). The absorption maximum is red-shifted to 373 nm in a basic NMP solution (Fig. 5b). Interestingly, when a few drops of the DAB-MWCNT in MSA solutions were added to pure NMP, the absorption peak red-shifted to 404 nm (Fig. 5a). The absorption maxima changes were closely related to the conjugation-length changes of the ground state in different solvents. In the two extreme cases, namely, in NMP and MSA solutions, this is clearly determined by the availability of the nitrogen lone–pair electrons of the DAB pendants to participate or not (Fig. 5c). In the intermediate case, the red-shift to 404 nm is rather surprising, suggesting even longer conjugation length and the possibility of extension into CNT framework. The emission maximum of DAB-MWCNT in MSA solution was 394 nm with a right shoulder peak at 415 nm (Fig. 5b). The solution emitted strong blue light when exposed to a hand-held UV light (365 nm) (Fig. 5b, inset). Similar to UV–vis absorption behavior, the sample in NMP solution shows that the peak red-shifted and centered at 421 nm with a right shoulder peak at 440 nm (Fig. 5b). In comparing with the spectrum of MSA solution, the peak maximum was shifted bathochromically by as much as 27 nm, implying that the electronic structure of the excited state had been affected by vastly different solvent environments. Surprisingly, the solution prepared from adding a few drops of DAB-MWCNT/MSA solution into pure NMP displayed a broader emission band with peak at 531 nm (Fig. 5b), showing a strong sky blue

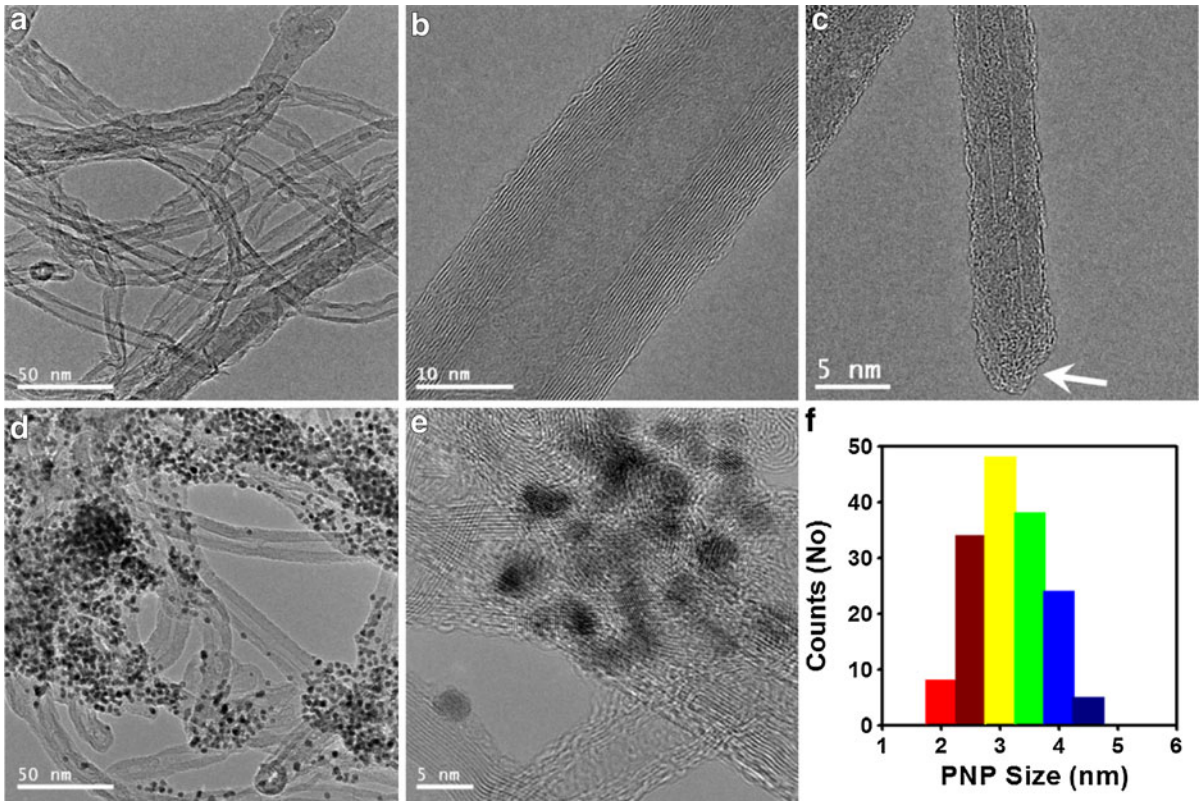

Fig. 4 TEM images of samples: **a**, **b** pristine MWCNT. **c** DAB-MWCNT, showing uniform decoration of DAB moiety onto the surface of MWCNT. **d**, **e** PNP/DAB-MWCNT. **f** the particle size distribution of PNP, which is uniform in the range of 3–5 nm

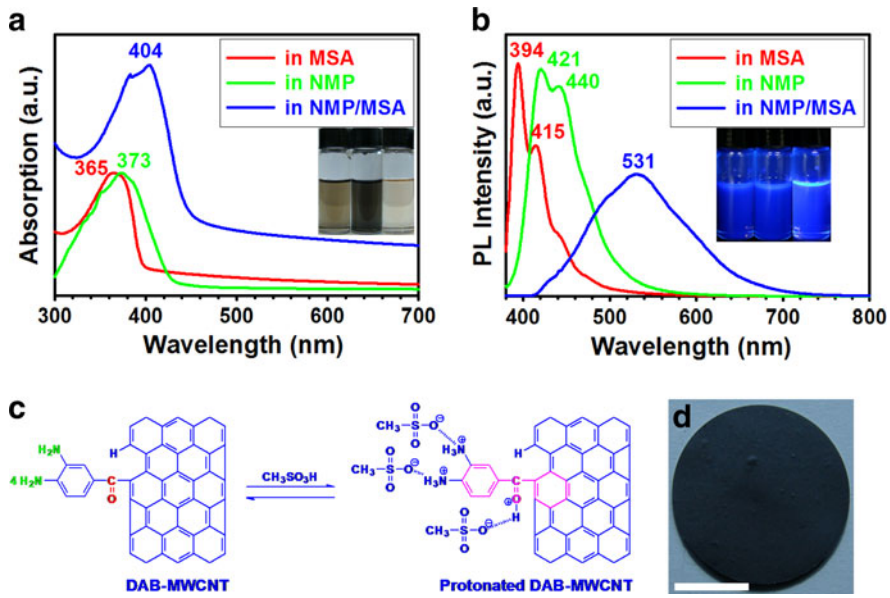

Fig. 5 **a** UV- vis absorption. **b** emission spectra of DAB-MWCNT solutions in MSA, NMP, and NMP with a few drops of MSA solution. *Inset* in (*a*) is photo of the solutions without hand-held UV lamp and *inset* in (*b*) is photo of the solutions with hand-held UV lamp (365 nm). The excitation wavelengths are UV–vis absorption maximum of each sample. **c** proposed charge complex formation of DAB-MWCNT in MSA solution. **d** DAB-MWCNT thin paper. *Scale bar* is 1 cm

fluorescence (Fig. 5b, inset). The emission peak was red-shifted by as much as 137 nm as compared to the spectrum of MSA solution. Similar to the UV absorption behavior, significant red-shifted emission maxima are related to extended conjugation lengths of charged complexes in NMP (Fig. 5c). Both UV–vis absorption and emission behaviors also strongly suggest that homogeneous dispersions of DAB-MWCNT can be achieved in organic solvents ranging from basic to acidic.

After homogeneous dispersion of DAB-MWCNT in MSA had been confirmed spectroscopically, the solution was cast on a leveled Petri dish and the MSA evaporated to produce DAB-MWCNT thin paper as described in the 'Experimental' section (Fig. 5d). The electrical conductivity of the resultant paper was measured by a standard four-point probe method under laboratory conditions. The average electrical conductivities of the paper were $280 \pm 8\ Sm^{-1}$, which is surprisingly better than the reported values for elastomer-nanotube thin films (Lahiff et al. 2006) or doped MWCNT-conjugated polymer films (Zhou et al. 2008). These results may be the best obtained so far for such a simple strategy, indicating that a relatively high loading of MWCNT has led to easy formation of a conduction network in the DBA-MWCNT thin paper, resulting in improved electrical properties.

By having numerous ortho-diaminobenzoyl units on the surface of DAB-MWCNT, PNP could be efficiently immobilized on the surface of the DAB-MWCNT to produce a PNP/DAB-MWCNT hybrid (Mandal et al. 2004). The DAB (o-diamine)–platinum chelate-type coordination bonding (Koizumi and Fukuju 2010) is expected to be stable, and thus, should display an enhanced electrochemical stability. Since PNP is aggregate-prone during an electrochemical reaction, the catalytic surface area is reduced (Yano et al. 2006). If CNT could provide a higher surface area to uniformly hold and immobilize PNP, then higher electrocatalytic activity may be possible (Laviron 1979a, 1979b). In this study, the amount of PNP loaded determined by TGA analysis was found to be ca. 13 wt% (Fig. 2b). The size distribution of PNP is uniform and in the range of 2–5 nm as determined by TEM (Fig. 4d–f). CV was performed in N_2- and O_2-saturated, 0.1 M aqueous KOH solutions in the potential ranging from −1.0 to 0.2 V versus Ag/AgCl and with a sweep rate of $10\ mV{\cdot}s^{-1}$. Hence, CV was used to estimate the electrocatalytic activity of the modified electrodes. For comparison, the CV curves were recorded for DAB-MWCNT and PNP/DAB-MWCNT on GC electrodes. DAB-MWCNT shows a featureless redox behavior in a N_2-saturated medium (Fig. 6a), while a weak reduction peak at −2.6 V in an O_2-saturated medium (Fig. 6b). PNP/DAB-MWCNT hybrid displays distinct reduction peaks at −0.16 and −0.14 V in both N_2- and O_2-saturated media, respectively, (Fig. 6a, b). Compared to DAB-MWCNT, the PNP/DAB-MWCNT hybrid shows significantly higher current and lower reduction potential, illustrating that the PNP/DAB-MWCNT electrode possesses much higher electrocatalytic activity and lower activation barrier for oxygen reduction reaction (ORR). For reference, CV curves for commercially available Vulcan XC-72R on GC electrodes, which displays higher current and reduction potential at −0.25 and −0.27 V, in both N_2- and O_2-saturated media, respectively, indicate that Vulcan XC-72R electrodes have higher electrocatalytic activity and activation barrier than the PNP/DAB-MWCNT electrodes. However, when taking into account the PNP contents of the PNP/DAB-MWCNT (13 wt%) and Vulcan XC-72R (20 wt%), electrocatalytic activities in a N_2-saturated medium are actually quite similar for both electrodes (Fig. 6c), the PNP/DAB-MWCNT electrode in an ORR condition is approximately 85% that of Vulcan XC-72R electrodes after 100 cycles (Fig. 6d). The current–time (i–t) responses for the sample electrodes clearly demonstrate current densities depending on cycle times (Fig. S2 in ESI). Together with current and potential values, the overall performance of PNP/DAB-MWCNT can be comparable with that of the optimized and commercially available Vulcan XC-72R.

In order to obtain an important electrocatalytic parameter during the ORR process, the reaction kinetics were investigated by rotating disk voltammetry (Fig. 7a). The voltammetric profiles showed that the current density was increased by increasing rotating rate. The onset potential of PNP/DAB-MWCNT/GC for ORR was about −0.12 V, which is close to that identified from CV measurements (Fig. 6b). The corresponding Koutecky–Levich curves at different electrode potentials revealed parallel plots with a good linearity (Fig. 7b), which are often taken as an indication of first-order reaction kinetics with respect to the concentration of dissolved O_2 (Bard and Faulkner 2001). The kinetic parameters

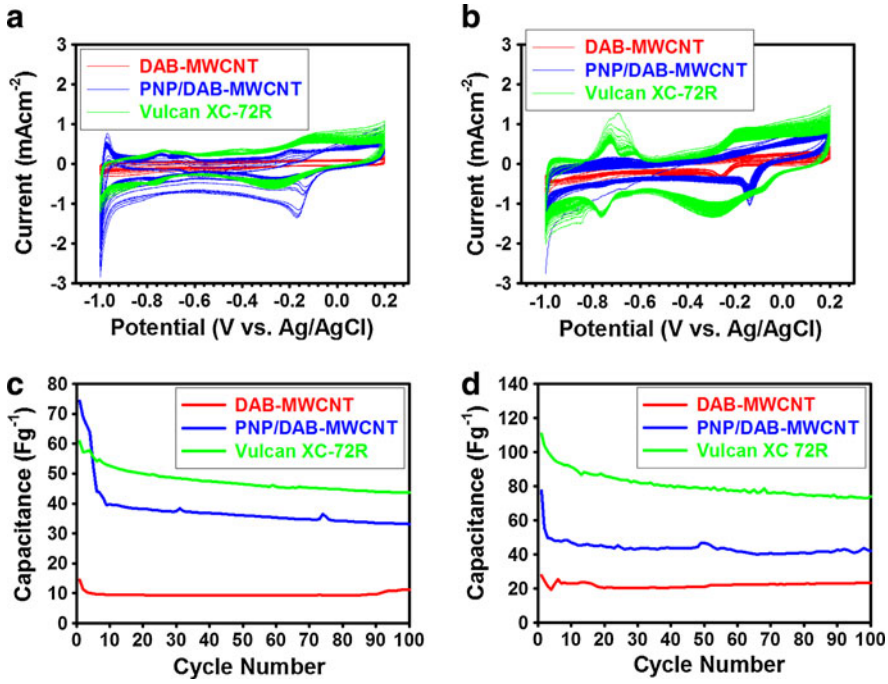

Fig. 6 CV curves of DAB-MWCNT/GC, PNP/DAB-MWCNT/GC, and Vulcan XC-72R/GC electrodes in 0.1 M aqueous KOH solution with a scan rate of 10 mVs^{-1}: **a** N_2-saturated medium. **b** O_2-saturated medium. **c** Electrochemical stability measurements of sample electrodes by means of sequential CV in N_2-saturated medium. **d** O_2-saturated medium

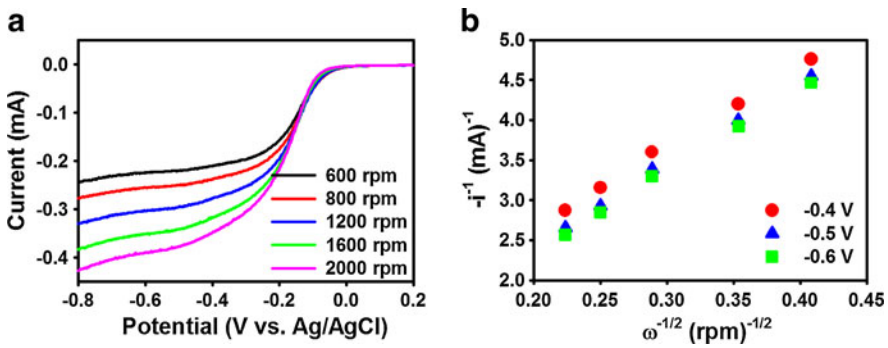

Fig. 7 **a** Rotating disk electrode (RDE) voltammograms of PNP/DAB-MWCNT/GC electrodes in an O_2-saturated 0.1 M aq. KOH solution with at different rotate rates of 600, 800, 1,200, 1,600, and 2,000 rpm. **b** Koutecky–Levich plots of the PNP/DAB-MWCNT derived from RDE measurements at different electrode potentials

can be analyzed on the basis of the Koutecky–Levich equation (Tammeveski et al. 1997). The transferred electron numbers per oxygen molecule involved in the oxygen reduction are 3.94, 3.91, and 3.89 at −0.4, −0.5, and −0.6 V, respectively, suggesting that the PNP/DAB-MWCNT leads to an efficient four-electron transfer in ORR process.

Conclusions

MWCNT was functionalized with DABA via a "direct" Friedel–Crafts acylation in a mildly acidic PPA/P_2O_5 medium. The resultant DAB-MWCNT was thoroughly characterized with EA, FT-IR, UV–vis, TGA, XRD, SEM, and TEM. The results showed that DAB moiety was introduced well onto the surface of DAB-MWCNT. In addition, XRD results showed that persisting metallic impurities in pristine MWCNT were mostly removed at the same time. The resultant DAB-MWCNT was used to support PNP to prepare a PNP/DAB-MWCNT hybrid, which was characterized, and an efficient deposition of PNP on DAB-MWCNT was confirmed. The morphology of the PNP/MB-MWCNT hybrid was studied with SEM and TEM, showing that PNP were uniformly distributed on the

surface of DAB-MWCNT. Compared to DAB-MWCNT, the PNP/DAB-MWCNT hybrid displayed distinct redox peaks with much higher electrocatalytic activity and lower activation barrier. The results suggest a new design of PNP/MWCNT-based electrocatalysts for energy conversion applications.

Acknowledgments This project was supported by funding from World Class University (WCU), US-Korea NBIT, and Basic Research Laboratory (BRL) programs supported by the National Research Foundation (NRF) and the Ministry of Education, Science and Technology (MEST) of Korea, US Air Force Office of Scientific Research, and Asian Office of Aerospace R&D (AFOSR-AOARD).

References

Ahmadi TS, Wang ZL, Green TC, Henglein A, El-Sayed MA (1996) Shape-controlled synthesis of colloidal platinum nanoparticles. Science 272(5270):1924

Alexeyeva N, Matisen L, Saar A, Laaksonen P, Kontturi K, Tammeveski K (2010) Kinetics of oxygen reduction on gold nanoparticle/multi-walled carbon nanotube hybrid electrodes in acid media. J Electroanal Chem 642(1):6–12

Baek JB, Lyons CB, Tan LS (2004) Covalent modification of vapour-grown carbon nanofibers via direct Friedel–Crafts acylation in polyphosphoric acid. J Mater Chem 14(13): 2052–2056

Bard AJ, Faulkner LR (2001) Electrochemical methods, fundamentals and applications. Wiley, New York

Carneiro O, Covas J, Bernardo C, Caldeira G, Van Hattum F, Ting JM, Alig R, Lake M (1998) Production and assessment of polycarbonate composites reinforced with vapour-grown carbon fibres. Compos Sci Technol 58(3–4):401–407

Charlier JC (2002) Defects in carbon nanotubes. Acc Chem Res 35(12):1063–1069

Chen GZ, Shaffer MSP, Coleby D, Dixon G, Zhou W, Fray D, Windle A (2000) Carbon nanotube and polypyrrole composites: coating and doping. Adv Mater 12(7):522–526

Dai L, Mau AWH (2001) Controlled synthesis and modification of carbon nanotubes and C 60: carbon nanostructures for advanced polymeric composite materials. Adv Mater 13(12–13):899–913

Eo SM, Oh SJ, Tan LS, Baek JB (2008) Poly (2,5-benzoxazole)/carbon nanotube composites via in situ polymerization of 3-amino-4-hydroxybenzoic acid hydrochloride in a mild poly (phosphoric acid). Eur Polym J 44(6):1603–1612

Han SW, Oh SJ, Tan LS, Baek JB (2008) One-pot purification and functionalization of single-walled carbon nanotubes in less-corrosive poly (phosphoric acid). Carbon 46(14):1841–1849

Heller DA, Barone PW, Strano MS (2005) Sonication-induced changes in chiral distribution: a complication in the use of single-walled carbon nanotube fluorescence for determining species distribution. Carbon 43(3):651–653

Hirsch A (2002) Functionalization of single walled carbon nanotubes. Angew Chem Int Ed 41(11):1853–1859

Hu H, Zhao B, Itkis ME, Haddon RC (2003) Nitric acid purification of single-walled carbon nanotubes. J Phys Chem B 107(50):13838–13842

Huang W, Lin Y, Taylor S, Gaillard J, Rao AM, Sun YP (2002) Sonication-assisted functionalization and solubilization of carbon nanotubes. Nano Lett 2(3):231–234

Jeon IY, Lee HJ, Choi YS, Tan LS, Baek JB (2008) Semimetallic transport in nanocomposites derived from grafting of linear and hyperbranched poly (phenylene sulfide) s onto the surface of functionalized multi-walled carbon nanotubes. Macromolecules 41(20):7423–7432

Kim SN, Slocik JM, Naik RR (2010) Strategy for the assembly of carbon nanotube-metal nanoparticle hybrids using bio-interfaces. Small 6:1992–1995

Koizumi T, Fukuju K (2010) Cyclometalated platinum (II) complexes bearing o-phenylenediamine derivatives: synthesis and electrochemical behavior. J Organomet Chem 696(6):1232–1235

Lahiff E, Leahy R, Coleman JN, Blau WJ (2006) Physical properties of novel free-standing polymer-nanotube thin films. Carbon 44(8):1525–1529

Laviron E (1979a) General expression of the linear potential sweep voltammogram in the case of diffusionless electrochemical systems. J Electroanal Chem 101(1):19–28

Laviron E (1979b) The use of linear potential sweep voltammetry and of ac voltammetry for the study of the surface electrochemical reaction of strongly adsorbed systems and of redox modified electrodes. J Electroanal Chem 100:263–270

Lee SY, Yamada M, Miyake M (2005) Synthesis of carbon nanotubes over gold nanoparticle supported catalysts. Carbon 43(13):2654–2663

Lee HJ, Han SW, Kwon YD, Tan LS, Baek JB (2008) Functionalization of multi-walled carbon nanotubes with various 4-substituted benzoic acids in mild polyphosphoric acid/phosphorous pentoxide. Carbon 46(14):1850–1859

Li J, Moskovits M, Haslett TL (1998) Nanoscale electroless metal deposition in aligned carbon nanotubes. Chem mater 10(7):1963–1967

Li W, Liang C, Zhou W, Qiu J, Zhou Z, Sun G, Xin Q (2003) Preparation and characterization of multiwalled carbon nanotube-supported platinum for cathode catalysts of direct methanol fuel cells. J Phys Chem B 107(26):6292–6299

Lorencon E, Ferlauto AS, de Oliveira S, Miquita DR, Resende RR, Lacerda RG, Ladeira LO (2009) Direct production of carbon nanotubes/metal nanoparticles hybrids from a redox reaction between metal ions and reduced carbon nanotubes. ACS Appl Mater Interfaces 1(10):2104–2106

Mandal S, Roy D, Chaudhari RV, Sastry M (2004) Pt and Pd nanoparticles immobilized on amine-functionalized zeolite: excellent catalysts for hydrogenation and heck reactions. Chem mater 16(19):3714–3724

Shaffer MSP, Windle AH (1999) Fabrication and characterization of carbon nanotube/poly (vinyl alcohol) composites. Adv Mater 11(11):937–941

Shi Y, Yang R, Yuet PK (2009) Easy decoration of carbon nanotubes with well dispersed gold nanoparticles and the use of the material as an electrocatalyst. Carbon 47(4): 1146–1151

Sun YP, Fu K, Lin Y, Huang W (2002) Functionalized carbon nanotubes: properties and applications. Acc Chem Res 35(12):1096–1104

Tammeveski K, Tenno T, Claret J, Ferrater C (1997) Electrochemical reduction of oxygen on thin-film Pt electrodes in 0.1 M KOH. Electrochim Acta 42(5):893–897

Tasis D, Tagmatarchis N, Bianco A, Prato M (2006) Chemistry of carbon nanotubes. Chem Rev 106(3):1105–1136

Wildgoose GG, Banks CE, Compton RG (2006) Metal nanoparticles and related materials supported on carbon nanotubes: methods and applications. Small 2(2):182–193

Wolfe JF (1988) Polybenzothiazoles and polybenzoxazoles. In Encyclopedia of polymer science and engineering, 2nd edn. Wiley, New York 11:601–635

Xue B, Chen P, Hong Q, Lin J, Tan KL (2001) Growth of Pd, Pt, Ag and Au nanoparticles on carbon nanotubes. J Mater Chem 11(9):2378–2381

Yano H, Inukai J, Uchida H, Watanabe M, Babu PK, Kobayashi T, Chung JH, Oldfield E, Wieckowski A (2006) Particle-size effect of nanoscale platinum catalysts in oxygen reduction reaction: an electrochemical and 195Pt EC-NMR study. Phys Chem Chem Phys 8(42):4932–4939

Yu R, Chen L, Liu Q, Lin J, Tan KL, Ng SC, Chan HSO, Xu GQ, Hor TSA (1998) Platinum deposition on carbon nanotubes via chemical modification. Chem mater 10(3):718–722

Zhang Y, Shi Z, Gu Z, Iijima S (2000) Structure modification of single-wall carbon nanotubes. Carbon 38(15):2055–2059

Zhou C, Wang S, Zhuang Q, Han Z (2008) Enhanced conductivity in polybenzoxazoles doped with carboxylated multi-walled carbon nanotubes. Carbon 46(9):1232–1240